SBGf19599

Multifocusing Stack – a New Time Imaging Method

Evgeny Landa, Boris Gurevich, Shemer Keydar, and Pinchas Trachtman

The Geophysical Institute of Israel

Abstract

The multifocusing method consists in stacking seismic data with arbitrary source-receiver distribution according to a new local moveout correction. This moveout correction is based on a local spherical approximation of the reflection wave front in the vicinity of an observation surface. We demonstrate that the multifocusing method does not require any knowledge of the subsurface model and can produce an accurate zero offset section, even in cases of a complex geological structure and low signal-to-noise ratio. The estimated sets of parameters, namely the emergence angle and the wave front curvatures for the normal wave and normal-incidence-point wave, which define the local moveout correction, contain important information regarding the subsurface model and may be used for structural and lithological inversion. We illustrate an application of the multifocusing imaging to synthetic data and compare it with conventional NMO + DMO stacking, prestack time and depth migrations.

INTRODUCTION

While depth imaging plays an increasing role in seismic data processing, imaging in time domain still remains an important exploration tool. Experience shows that time imaging provides sufficient information for a variety of subsurface models of moderate complexity. Moreover, even for more complex models that warrant the use of prestack depth migration, time imaging usually constitutes a key first step, which facilitates the estimation of the macro-velocity model for depth imaging.

For these reasons improving the quality of time sections remains the focus of intensive research. In particular, a lot of efforts are directed towards improving the accuracy and reliability of stacking procedures (de Bazailere, 1988; Tygel et al., 1997). The most systematic approach to zero-offset imaging and stacking is called multifocusing.

The multifocusing method is a new stacking procedure proposed by Boris Gelchinsky (Gelchinsky et al., 1997; Berkovitch et al., 1998). In multifocusing, each image trace is constructed by stacking an arbitrary number of seismic traces which need not belong to the same CMP gather, but whose sources and receivers are within a certain vicinity of the image point. Since the traces being stacked no longer belong to the same CMP gather, such a procedure requires a more general moveout correction than the one used in the conventional CMP stacking. Analytical expressions (based on the spherical representation of wavefronts) describe the moveout correction for a given source-receiver pair with respect to a zero-offset image trace by three parameters measured at the image point. In other words, the moveout correction expressed by the multifocusing formulas is a three- parameter expansion of the traveltime in the vicinity of the image point. In this sense it is closely related to the paraxial ray approximation (see e.g. Tygel et al., 1997). The three parameters are: the emergence angle β and the radii of curvature R_{NIP} and R_N of two fundamental wave fronts. The Normal-Incidence-Point (NIP) (or common-reflection-element) wave front is formed by a point source placed at the point where the zero-offset ray emitted from the image point hits the reflector. The wavefront of the Normal (N) wave (common - evolute - element front) is formed by normal rays emitted by different points on the reflector (like in an "exploding reflector" scenario).

It has been shown that the multifocusing formulas not only provide an adequate representation of the arrival times for arbitrary source-receiver configurations just like the conventional NMO correction does for CMP gathers, but is in fact more accurate for various earth models. In particular, the multifocusing formulas are very accurate for a spherical reflector under a homogeneous overburden, and for a smoothly curved dome-like reflector (Tygel et al., 1997).

For a single CMP gather the multifocusing moveout correction reduces to the "shifted hyperbola" of de Bazelaire (1989), which is known to give a superior approximation of the traveltimes for a horizontally layered medium than the classical Dix NMO equation (Castle, 1994).

MULTIFOCUSING MOVEOUT CORRECTION

Let us consider the ray diagram in Figure 1. The central ray starts at point X_0 with angle β to the vertical, hits the reflector Σ at NIP and returns again at X_0. A paraxial ray from the source S intersects the central ray at point P and arrives back to the surface at point G. These two rays define a fictitious focusing wave which starts with the wave front Σ_S, focuses at P, is reflected at the reflector Σ, and emerges again at X_0 with the wave front Σ_G. Following the formulas of Gelchinsky et al. (1997), we can write the expression for moveout correction in the form (Berkovitch et al., 1998):

$$\Delta\tau = \frac{\sqrt{(R^+)^2 + 2R^+\Delta X^+ \sin\beta + (\Delta X^+)^2} - R^+}{V_0} + \frac{\sqrt{(R^-)^2 + 2R^-\Delta X^- \sin\beta + (\Delta X^-)^2} - R^-}{V_0} \quad (1)$$

where

$$R^{\pm} = \frac{1 \pm \sigma}{\dfrac{1}{R_N} \pm \dfrac{\sigma}{R_{NIP}}},$$

and σ is the so-called focusing parameter given by

$$\sigma = \frac{\Delta X^+ - \Delta X^-}{\Delta X^+ + \Delta X^- + 2\dfrac{\Delta X^+ \Delta X^-}{R_{NIP}} \sin\beta},$$

where ΔX^+ and ΔX^- are the source and receiver offsets of an arbitrary ray with respect to the central ray, R^+ and R^- are the wave front curvatures of the fictitious waves Σ_S and Σ_G, respectively, and V_0 is the near surface velocity.

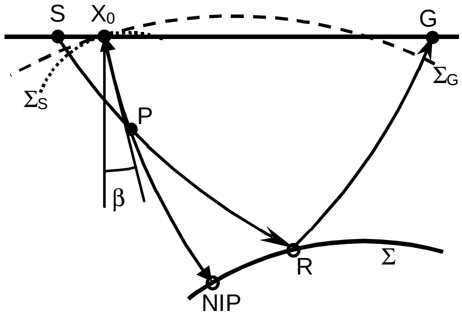

Figure 1: Ray diagram showing the construction of the focusing wave

ADVANTAGES OF MULTIFOCUSING

Potential benefits of the multifocusing as compared to the more traditional methods of time imaging (NMO+DMO) can be described as follows:

- Stacking large number of traces belonging to different CMP gathers can increase signal-to-noise ratio by attenuating noise originating at a target depth.
- For a flat reflector under a homogeneous overburden the NIP radius depends on the distance between the image point and the reflector and is independent of the reflector dip. For an inhomogeneous overburden R_{NIP} represents the distance between the image point and the reflector in a reference medium (homogeneous medium with reference velocity V_0 equal to the velocity in the uppermost layer near the observation surface), again, irrespective of their dip. Therefore, the events with similar t_0 beneath the same overburden have similar R_{NIP} values irrespective of their dip. Thus, the multifocusing imaging based on the radii of curvature preserves dipping events. In this respect the multifocusing method incorporates the key property of the DMO transform.

- Simultaneous determination of the curvatures and emergence angle makes it possible to recover dip independent RMS velocities V_{RMS} through a simple algebraic transformation,

$$V_{RMS} = \left(\frac{2V_0 R_{NIP}}{t_0}\right)^{1/2},$$

  where t_0 is the zero-offset arrival time at the image point. These velocities may be then used for migration.
- The multifocusing moveout correction for a given sample of the image trace at t_0 depends on the incidence angle and on curvatures measured on seismograms, and does not involve the value of t_0 itself. Thus all samples belonging to the same event would have the same parameters and hence the same moveout correction. Thus, the multifocusing moveout correction does not cause stretch of the signal.

IMPLEMENTATION

The combination of the generality and accuracy makes the multifocusing formulas an appealing basis for an imaging procedure. However, despite the potential advantages of the multifocusing approach its practical use in processing of real data has been held back partly by the difficulties of implementation. Indeed, implementation of the multifocusing method has an inherent difficulty associated with the need to determine, for each t_0 on each image trace, three imaging parameters: β, R_{NIP} and R_N instead of a single parameter (stacking velocity) in the conventional NMO stack. For the NMO stack the stacking velocity is usually determined by means of the interactive velocity analysis, consisting in displaying a panel of correlation measure (e.g., semblance) as a function of t_0 and velocity, and manual picking of the appropriate correlation maxima as a function of t_0. For the multifocusing parameters a similar procedure is out of the question for two reasons. First, the cost of calculating the correlation measure for all possible combinations of three parameters over a large gather of traces is prohibitively high. Secondly, even if such computation was possible, an interactive procedure would have to involve displaying and picking maxima of the correlation measure as a function of four variables (t_0 and three imaging parameters), which does not look practical.

Thus, the determination of the imaging parameters must involve some kind of automation based on automatic optimization methods. This, in turn, brings about all sorts of problems associated with automatic correlation/stacking procedures, which have been encountered before in numerous attempts to construct an automatic NMO stack. A basic problem here is that automatic imaging procedures optimally stack useful signal as well as noise, especially spatially correlated noise. The correlation measure as a function of parameters may not be unimodal, thus requiring a global optimization strategy. However, even the global maximum may be related to the noise rather than to the signal. For example, strong multiple reflections may have higher correlation measure than weaker primary events. In the interactive correlation procedures this ambiguity is resolved manually by picking right maxima on the basis of a priori velocity information. In the automatic procedure the only way is to impose constraints on the imaging parameters. Such a constrained optimization procedure has been employed in our implementation of the multifocusing method.

Implementation of the multifocusing method is based on a phase correlation of the signal on the observed seismic traces. The data are moveout corrected along different travel time curves to find the curve closest to the travel time curve of the signal. The unknown parameters β, R_{NIP}, and R_N are estimated by finding a set of parameters which maximizes the semblance function. Semblance is calculated over the multifocusing gather in a time window along the trial travel time curve. Maximization of the semblance is achieved by a nonlinear global optimization method.

The correlation procedure described above is repeated for each central image point and for each time sample forming a multifocusing time section. Each sample on this section represents the optimal stacked value corresponding to the optimal parameters of β, R_{NIP} and R_N and it is close to an accurate zero-offset section. Estimated sets of parameters can also be represented in the time section forming so-called anglegram $\beta(x,t_0)$ and radius-grams $\beta(x,t_0)$, $R_{NIP}(x,t_0)$, and $R_N(x,t_0)$. These three additional sections provide new physically sound wavefield attributes which may aid the interpretation and inversion.

EXAMPLE

Here the application of multifocusing is demonstrated on a Land dataset from Canadian foothills donated by Husky Oil for use in an SEG convention workshop. Figure 2 shows a conventional CMP stacked section obtained after a detailed velocity analysis and DMO. Figure 3 shows the multifocusing stacked section. One can see a substantial improvement over the conventional section. This improvement can be explained as follows.

The conventional stacked section has rather low signal-to-noise ratio, especially in the upper part. This was probably caused by a rather small fold in the data. Indeed, this is a 2D line from a 3D dataset, that's why it has only a fold of 30. Figure 4 shows nine CMP gathers 30 traces per gather. For the conventional NMO-DMO stack each of these gathers is individually stacked after NMO and DMO.

For the multifocusing approach, these gathers are combined into a single MF gather. Such a gather, consisting now of 280 traces is shown in Figure 5 (left). The right panel of Figure 5 shows the same MF gather after the application of the multifocusing moveout correction. One can observe a nearly perfect alignment of many reflection events. Flattening of

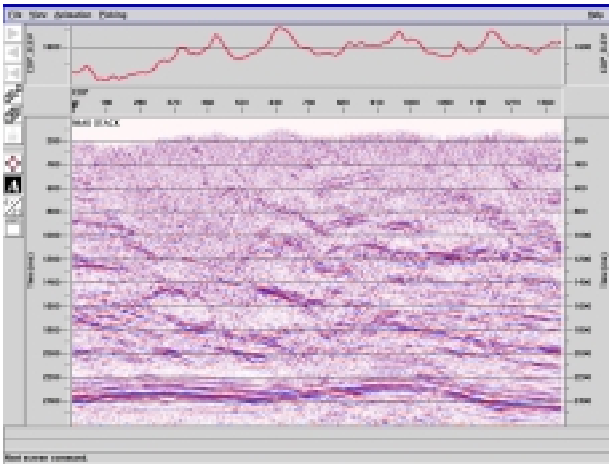

Figure 2: Conventional NMO+DMO stacked section

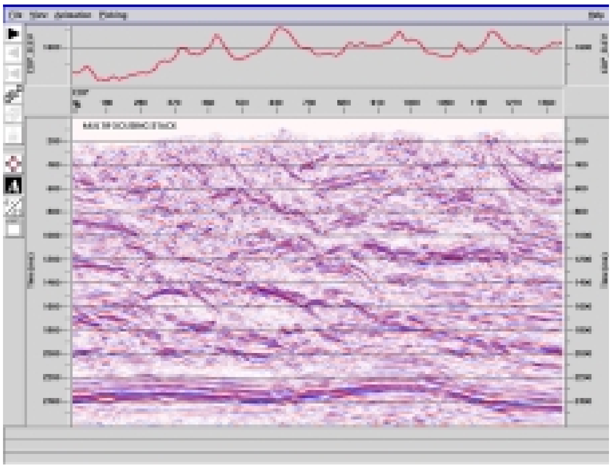

Figure 3: Multifocusing time section

such a huge gather which spans over many CMPs was achieved after the *automatic* multifocusing parameter estimation. This procedure is illustrated by Figure 6.

In this figure, the central panel shows the correlation measure (semblance) as a function of t_0 and emergence angle. Areas of high semblance correspond to the dips visible on a fragment of the stacked section (right panel). The left panel shows the curvature radius of the NIP wave front as a function of t_0 and angle. Such panels are used for quality control only and are shown here just to illustrate the procedure performed automatically by the multifocusing software to find the set of optimal moveout parameters. These parameters are then utilized in the multifocusing moveout correction, which is applied to each multifocusing gather. This ensures an increase of the stacking power of multifocusing over a conventional stack by a factor of eight!

CONCLUSIONS

We implemented a new multi-coverage time imaging method called multifocusing. The multifocusing method consists in stacking seismic data with arbitrary source-receiver distribution according to a new local moveout correction. We have demonstrated that the multifocusing method can produce a zero offset section superior to the NMO/DMO stacked section in an automatic manner even in cases of a complex geological structure. The method is particularly useful for the situations of low fold and/or low signal-to-noise ratio. The estimated sets of multifocusing parameters, namely the emergence angle and the wave front curvatures for normal wave and normal-incidence-point wave, provide new physically founded wavefield attributes that may be useful for the interpretation and inversion.

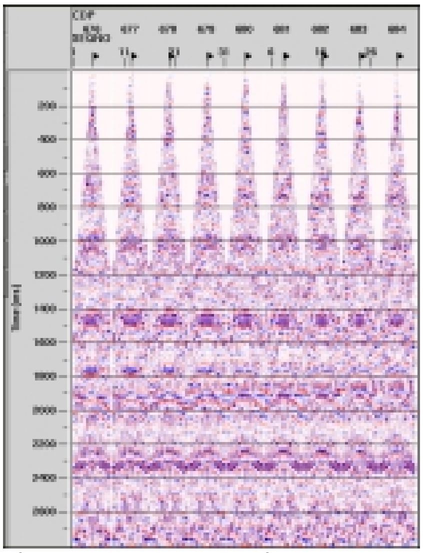

Figure 4: Input CMP gathers

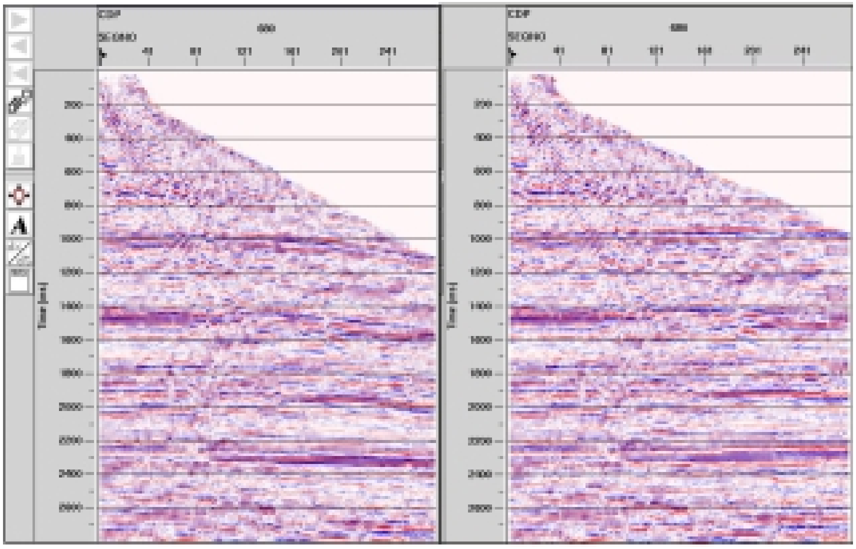

Figure 5: Left: MF gather, right: the same MF gather after the multifocusing moveout correction

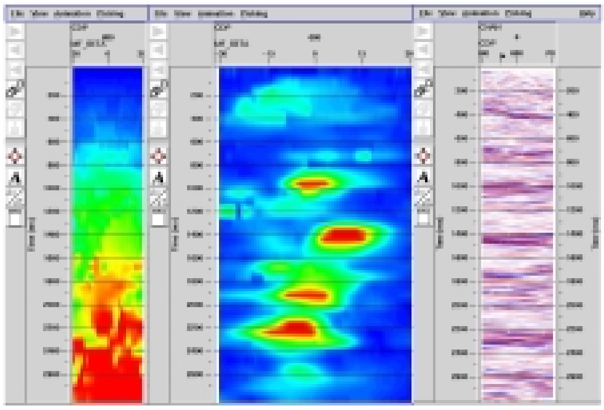

Figure 6: Panels illustrating automatic multifocusing parameter estimation

REFERENCES

de Bazelaire, E., 1988, Normal moveout correction revisited: Inhomogeneous media and curved interfaces, Geophysics, ***53****, 143-157.*

Berkovitch, A., Keydar, S., Landa, E., and Trachtman, P, 1998, Multifocusing in Practice, 68^{th} Annual Meeting, Society of Exploration Geophysicists, Expanded Abstracts.

Castle, R., 1994, A theory of normal moveout, Geophysics, ***59****, 983-999.*

Gelchinsky, B., Berkovitch, A., and Keydar, S., 1997, Multifocusing Homeomorphic Imaging: Part 1: Basic concepts and formulae,:Presented at the special course on Homeomorphic Imaging by B. Gelchinsky, Seeheim, Germany.

Tygel, M., Muller, Th., Hubral, P., and Schleicher, J., 1997, Eigenwave based multi-parameter traveltime expansions, 67^{th} Annual Meeting, Society of Exploration Geophysicists, Expanded Abstracts, 1770-1773.

ACKNOWLEDGMENTS

Special thanks go to Moshe Reshef of Landmark for his contribution to the software development. The authors acknowledge the financial support of the European Commission through Joule Programme.